Journal of Defence and Security Industries: Strategy and Technology, *2026*, *1(1)*

Science & Technology Section

Comparison of Powder Mixing Methods for Metal Matrix Composite Powders Used in Laser Powder Bed Fusion

Gökhan Dursun [1,*], Dilara Çelik [1], Yağmur Can Gündoğan [1], İrem Bal [1]

Abstract

Metal Matrix Composites (MMCs) reinforced with ceramic particles provide enhanced mechanical properties for high-performance applications. Accordingly, Laser Powder Bed Fusion (LPBF) enables the fabrication of complex and lightweight structures from these materials. However, achieving a homogeneous particle distribution within metal matrix remains a key challenge while maintaining powder processability. In this work, we investigated different powder mixing techniques: acoustic, tumbler, and ball milling for dispersing TiC ceramic particles into Inconel 625 powders. Micro- and nano-sized particles were systematically studied to examine the effect of particle size on the reinforcement distribution within the matrix during powder preparation. The objective was to achieve homogeneous dispersion of reinforcement particles within the Inconel 625 while preserving the spherical morphology of matrix powders. Powder characteristics such as flowability, apparent density, and tap density with respect to particle size, content and mixing parameters for each method were analysed. Results revealed that the acoustic mixing achieved uniform dispersion of TiC particles with minimal agglomeration and maintained the spherical shape of the matrix powders. In comparison, ball milling resulted in surface deformation and particle clustering in mixed powders, whereas tumbler mixing caused significant agglomeration of the reinforcements. The addition of TiC particles and applied mixing methods led to slight decrease in flowability of the composite powders due to increased surface roughness. Among all methods, powders prepared with acoustic system showed superior flow behaviour and the lowest Hausner ratio. Furthermore, fully dense samples were successfully produced using the powders processed via acoustic mixer, confirming their suitability for LPBF processing. This study demonstrated the potential use of acoustic mixing as an efficient and scalable method to produce high-quality MMC powders with improved dispersion while fulfilling the requirements of LPBF process.

Keywords: metal matrix composites, laser powder bed fusion, additive manufacturing, powder mixing.

Received: 13.11.2025 Accepted: 24.12.2025 Research Article

[1] TUSAS Engine Industries Inc., Eskişehir, Türkiye
* Corresponding author.
✉ gokhan.dursun@tei.com.tr

Cite this article as: Dursun, G., Celik, D., Gundogan, Y.C., & Bal, İ. (2025). Comparison of powder mixing methods for metal matrix composite powders used in laser powder bed fusion. *Journal of Defence and Security Industry: Strategy and Technology 1*, 154-174.

1. Introduction

The Metal Matrix Composites (MMCs) belong to a class of advanced materials with improved mechanical and physical properties, derived from the integration of reinforcements with distinctive individual properties. These include enhanced strength, stiffness, reduced density, improved hardness, and superior wear resistance (Tjong, 2007). Ductile alloys are commonly used as matrix materials to combine with reinforcements, which typically exhibit low thermal expansion and advanced toughness (Parsons & Shaik, 2022). Although MMCs present noticeable advantages in thermomechanical properties compared to their pure alloy forms, they still have gained limited acceptance in industry. Thus, MMCs have significant potential for wide range of application within various sectors.

The fabrication methods for MMCs include stir casting, powder metallurgy, and additive manufacturing. However, most traditional techniques result in high cost and mostly limits the geometrical complexity. Therefore, Additive Manufacturing (AM) in MMCs fabrication presents outstanding capability for complicated parts and will gradually involve the adoption of MMCs in industry thanks to the advantages offered by AM technologies. Among the AM techniques, Laser Powder Bed Fusion (LPBF) has emerged as the leading technology for fabricating MMCs. The operation principle for is LPBF based on layer-by-layer processing. A thin layer of powder is spread uniformly onto a substrate and then is partially fused by a high-energy input, usually either a laser or electron beam.

It is well known that characteristics and composition of feedstock powders have a major effect on material properties of final parts produced by LPBF (Murray, et al., 2019). Apparent density, flowability, morphology, and particle size basically control the powder behaviour during processing. From this perspective, there are various studies that investigate the powder quality and its effects on material properties of components. Liu, et al. (2011) demonstrated that an increase in the fraction of fine particles in 316L stainless steel powders allows higher density of parts in addition to enhancing the surface quality. Similarly, Baitimerov, et al. (2018) investigated different batches of gas atomized powders from different manufacturers and found that powder flowability and apparent density have an effect on the processability and eventually lead variation in microstructure and porosity in specimens. It has also been determined that powder flowability is enhanced with spherical particles which ultimately ensures the quality of LPBF parts (Niu & Chang, 1999).

In MMCs, material properties of the fabricated components strongly depend on parameters related to the size, type and concentration of reinforcement, in addition to powder mixing methods (Baitimerov et al., 2018). In addition, inappropriate powder properties might lead to undesirable defects such as increased porosity or void formation within manufactured parts, thus compromising their structural integrity.

Ball milling is one of the methods that allows wet or dry grinding of materials, mechanical alloying and homogeneous mixing using impact force. This process is carried out as a result of the interaction between chamber and balls. In this process, mixing is carried out by providing centrifugal movement within the determined parameters such as rotation speed, time, number of repetitions. Gu et al. (2009) applied high-energy mechanical alloying to Ti-Al-graphite powder mixtures and achieved morphological evolution from flattened to coarsened spherical shapes with increasing milling time. In another study, conducted by Zhuang et al. (2020), nanocomposite powders prepared using planetary ball milling was investigated and found that prolonged milling time causes undesirable clustering of reinforcement particles. Meanwhile, Yang et al. (2022) investigated the ball milling technique under different conditions, including dry, wet, and hollow ball milling. They concluded that powder sphericity is damaged with the long dry ball milling time while wet ball milling cannot ensure the particles to be welded. These studies further highlight the complexities involved in achieving optimal dispersion of reinforcements through ball milling.

Tumbler mixing is another widely used method in composite powder preparation. The three-dimensional rotational motion in the tumbler mixing offers minimizing the mechanical deformation of metallic powders and allows powder mixing without agglomeration. The composite powder preparation of 316L stainless steel reinforced with Y_2O_3 nanoparticles was carried out using tumbler mixing. It was observed that tumbler mixing can result in rough particle surfaces, which ultimately lead to reduced powder flowability during the LPBF process (Zhai, et al., 2020). Similarly, this technique was also employed for preparing Inconel 718 powder reinforced with TiC nanoparticles and revealed that constituents are dispersed uniformly within the matrix (Yao, et al., 2017). However, this method typically requires a long processing time to prepare the composite powder, which is considered a significant drawback for industrial applications (Dadbakhsh et al., 2020).

Even though different powder mixing methods are available in industrial applications, resonant acoustic mixing (RAM) has emerged as an innovative technique by offering uniform dispersion, minimizing agglomeration, and maintaining powder flow properties. RAM is known for its ability to achieve rapid and uniform mixing via of low-frequency energy. It generates acoustic interaction and unique material movement inside the chamber. Specifically, RAM mixers control vertical motion to induce vibration and movement of the resonator plate, thereby transferring energy to the contents within the mixing vessel. Compared to traditional mechanical mixers, RAM technology combines low-frequency, high-intensity motion with the acoustic energy. Smith et al. (2020) demonstrated that efficient mixing of Y_2O_3-coated NiCoCr composite powders can be achieved using RAM technology. Similarly, in another study, RAM was used to mix carbon nanotubes (CNTs) with AlSi10Mg in order to attain uniform particle dispersion (Thompson et al., 2019).

This research conducts a systematic study for comparison of composite powder preparation techniques, namely, high-energy ball milling, tumbler mixing, and resonant acoustic mixing. A detailed and systematic analysis of powder morphology, apparent density, and flowability was conducted for Inconel 625 alloy reinforced with micro- and nano-sized TiC particles. The objective was to determine an optimal composite powder preparation strategy for LPBF technology that ensures both homogeneity and processability across different reinforcement particle sizes.

2. Methodology

Gas-atomized Inconel 625 powder, with an average particle size of 35 µm, was employed as the matrix alloy in this study (Figure 1). TiC reinforcements were introduced at a fixed content of 2 wt% in two size ranges: nano-sized particles (35–55 nm) and micro-sized particles (1–10 µm). The composite powders were mixed using three different techniques: acoustic mixing, high-energy ball milling, and a tumbler system. The process parameters for each mixing method were investigated and optimized to achieve a uniform distribution of TiC particles within the matrix. LPBF process parameters were adopted from literature optimized for Inconel alloy as shown in Table 1 (Poyraz & Kushan, 2019).

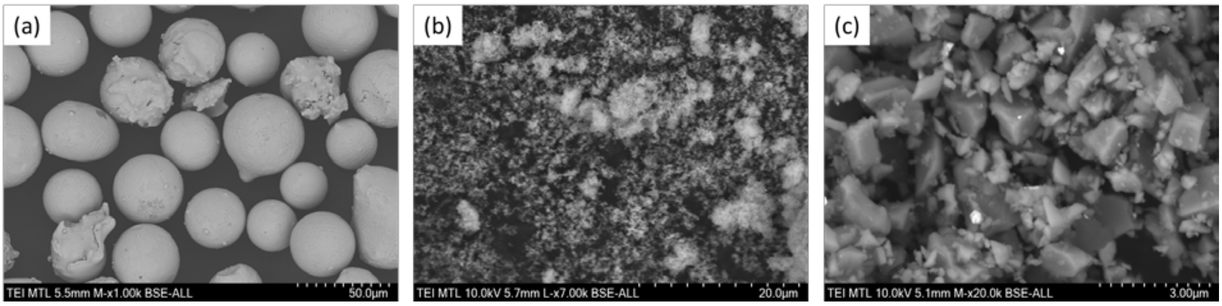

Figure 1. SEM images of (a) Virgin Inconel 625 particles (matrix), (b) Nano-sized TiC particles, and (c) Micro-sized TiC particles.

Table 1. LPBF process parameters (Poyraz & Kushan, 2019).

Laser power (W)	285
Laser scanning speed (mm/s)	960
Hatch distance (mm)	0.11
Layer thickness (mm)	0.040

2.1. Preparation of Powder Mixtures

2.1.1. Ball Mill Mixing

Planetary Mono Mill Pulverisette 6 classic line device was used for ball milling process. Dry mixing was performed in a ZrO_2 chamber with ZrO_2 grinding balls, maintaining a ball-to-powder mass ratio of 1:1. The mixing parameters are summarized in Table 2. To prevent excessive heating, 10 min cooling period was applied after every 15 min of milling. These parameters were independently applied to mix both micro-sized and nano-sized TiC particles with the Inconel 625 matrix powder.

Table 2. The parameters of the mixture experiments for ball milling.

Time (min)	Rotation speed (rpm)
60	150 300
120	150 300
180	150 300

2.1.2. Tumbler Mixing

The tumbler mixing process was carried out using a Turbula T2F device. The rotational speed was adjusted by changing the position of the drive belts on the five-stage pulley system, enabling a velocity range of 23–101 rpm. The experimental setup employed 2 wt% micro- and nano-sized TiC particles as reinforcements. TiC/Inconel 625 composite powders were mixed for durations of 4, 8, and 12 h at a constant rotational speed of 101 rpm. A 2000 mL cylindrical plastic vessel was used with a fill level of 50%. The complete set of experimental parameters is summarized in Table 3.

Table 3. Tumbler mixing parameters for tumbler mixing.

	2 wt% micro-sized TiC	2 wt% nano-sized TiC
Mixing time (h)	4, 8, 12	4, 8, 12
Fill level (%)	50%	50%
Rotational Speed (RPM)	101	101

2.1.3. Resonant Acoustic Mixing (RAM)

The Resodyn LabRAM II device was used for the RAM method. The vertical movement of the resonator plate and the attached vessel holder generate acoustic energy, which induces dispersion of reinforcement within matrix. To maintain the desired outcomes and ensure a safe mixing environment, powders were added to the system in accordance with specific weight limits. The container was periodically cooled during the mixing process to prevent powder agglomeration due to the risk of the excessive heating. The RAM device has 1 kg mixing capacity and can deliver up to 100 g acceleration for effective processing. In the experimental procedure, 2 wt% micro-sized TiC was first introduced into the container and mixed at 90 g for 1 min. Following this, the matrix powder was added and mixed at 80 g for durations ranging from 1 to 4 min. A similar procedure was applied for 2 wt% nano-sized TiC particles, with mixing times ranging from 1 to 6 min. The experimental setup for the acoustic mixer is shown in Table 4.

Table 4. Experimental parameters for resonant acoustic mixing.

	Micro-sized TiC	Nano-sized TiC
Mixing time (min)	1-4	1-6
Fill ratio (%)	80	80
G-force	80	80

2.2. Characterization

Morphology, particle size, shape, and distribution of the composite powders were characterized using Hitachi SU5000 scanning electron microscope (SEM) equipped with an energy-dispersive spectroscopy (EDS) system. Flow rate measurements of the composite powders were carried out using the PowderFlow Measurement Kit in accordance with ASTM B213 and ASTM B964. Hall flow tests were conducted with 50.0 g of powder, while Carney flow tests used 150.0 g in accordance with ASTM B213 and ASTM B964 standards. Apparent density was determined using 25 cm^3 of powder via the PowderFlow Measurement Kit, following ASTM B212 and ASTM B417 standards. Tapped density measurements were performed with 100.0 g of powder using a Torontech Tap Density Tester in accordance with ASTM B527. Flow properties were evaluated by calculating the Hausner ratio from the apparent and tapped density results. SEM was also used to analyse the microstructure of the bulk samples. The specimens were sectioned along the XY-plane using electrical discharge machining (EDM), mounted within a polymer (Bakelite) holder, and subsequently ground, polished, and etched using a glycaemia solution.

3. Results

The Inconel 625 matrix alloy was analysed using SEM, as shown in Figure1a, revealing that the matrix powders mainly had a spherical morphology, with minor irregularities. EDS analysis confirmed the presence of the expected elements in the Inconel 625. Figure 1b presents SEM images of the nano-sized TiC particles, which exhibited slight agglomeration due to their nanoscale size. Figure 1c presents SEM images of the micro-sized TiC particles, which exhibit an irregular and non-spherical shape form. The matrix powder (as shown in Table 5) exhibited an apparent density of 4.616 g/cm^3 and a tapped density of 5.264 g/cm^3. The resulting Hausner ratio was 1.14, while the Hall flow rate was measured as 17.106 s, both of which indicate good powder flowability. Distribution of reinforcement in Inconel 625 powder

Figure 2 presents SEM images of the composite powder reinforced with 2 wt% micro-sized TiC, prepared by the ball milling method. The results reveal that TiC particles caused noticeable deterioration in the surface texture and morphology of Inconel 625 particles, attributed to mechanical impact from the ceramic particles during milling. Similarly, Figure 3 illustrates the morphology of the 2 wt.% nano-sized TiC particles-reinforced powder, which exhibited comparable surface damage and a higher degree of particle adhesion. A homogeneous distribution of TiC particles was not achieved; instead, both nano- and micro-sized TiC reinforcements formed localized agglomerates, indicating limited dispersion. Furthermore, increasing the milling time and rotational speed did not effectively suppress agglomeration. Among all tested parameters, the most favourable results for the ball milling technique were obtained at 150 rpm for 180 min for both nano- and micro-sized powders.

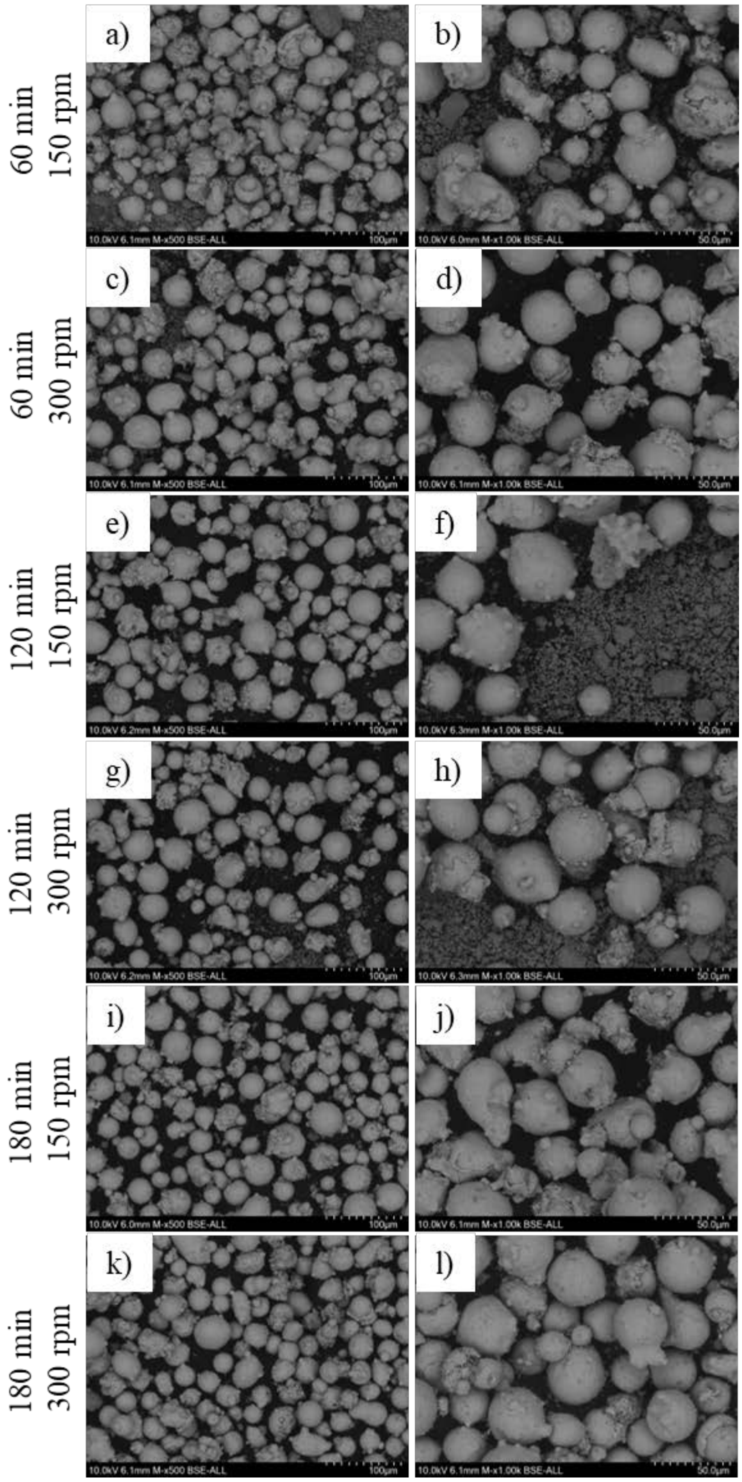

Figure 2. SEM micrographs of the 2 wt% micro-size TiC particles-reinforced Inconel 625 composite powders processed via ball milling at different magnifications with (a), (b) for 60 min 150 rpm; (c), (d) for 60 min 300 rpm; (e), (f) for 120 min 150 rpm; (g), (h) for 120 min 300 rpm; (i), (j) for 180 min 150 rpm; (k), (l) for 180 min and 300 rpm.

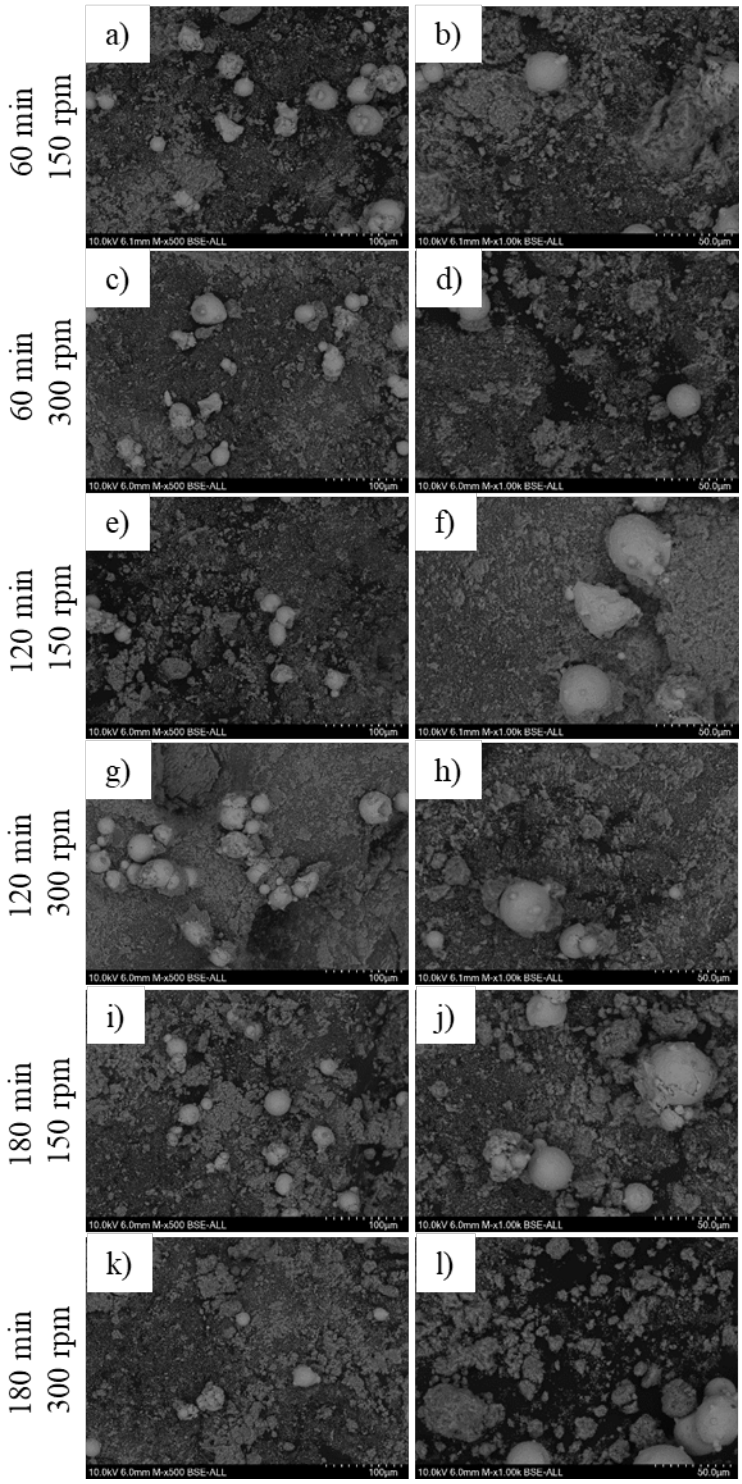

Figure 3. SEM micrographs of the 2 wt% nano-sized TiC particles-reinforced Inconel 625 composite powders processed via ball milling at different magnifications with (a), (b) for 60 min 150 rpm; (c), (d) for 60 min 300 rpm; (e), (f) for 120 min 150 rpm; (g), (h) for 120 min 300 rpm; (i), (j) for 180 min 150 rpm; (k), (l) for 180 min and 300 rpm.

In Figure 4, SEM images of the powder mixture composed of nano-sized TiC reinforcement particles prepared using a tumbler mixer are presented. As shown in Figure 4, majority of the nano-sized particles did not adhere to the matrix powders, and a significant agglomeration was observed. This indicates that a 4 h mixing duration is insufficient to achieve effective dispersion of the reinforcement particles. Although some matrix particles were partially coated with reinforcement particles, remaining powders exhibited minimal adhesion, resulting in an inconsistent and non-uniform mixture. To further evaluate the effect of mixing time, SEM images were analysed after 8 and 12 h of mixing. However, no significant improvement in the homogeneity of the nano-sized particles was observed, even with extended mixing durations.

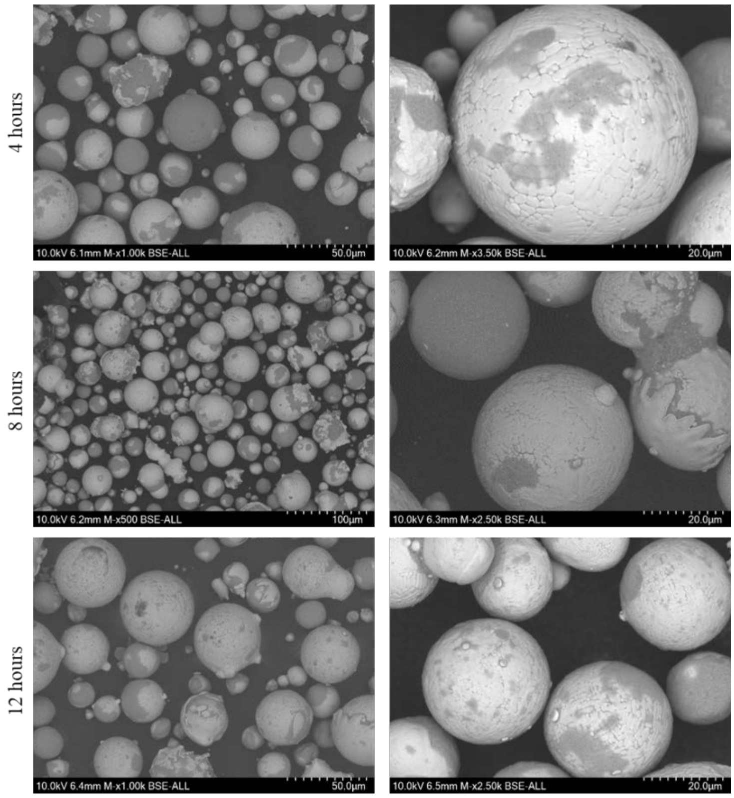

Figure 4. SEM images of 2 wt% nano-sized TiC/Inconel 625 composite powder from the different mixing time and magnification (Turbula system).

In the case of micro-sized TiC particles, Inconel 625 processed using the tumbler mixer, SEM images in Figure 5 reveals that poor dispersion of the reinforcement particles after 4 h of mixing, with visible clusters and agglomerates. The surfaces of the Inconel 625 powders remained largely uncoated, as the relatively larger micro-sized TiC particles tended to remain embedded within the matrix. However, a significant improvement in particle distribution and interfacial adhesion was observed with extended mixing times. After 8 h, particle clustering was noticeably reduced, and a more uniform distribution across the matrix was achieved, indicating an improvement in mixture homogeneity due to prolonged mechanical interaction. Further enhancement was observed after 12 h of mixing, where clustering was minimized and a more consistent, homogeneous dispersion was achieved. These findings highlight the critical influence of both particle size and mixing duration on the homogeneity of composite powders.

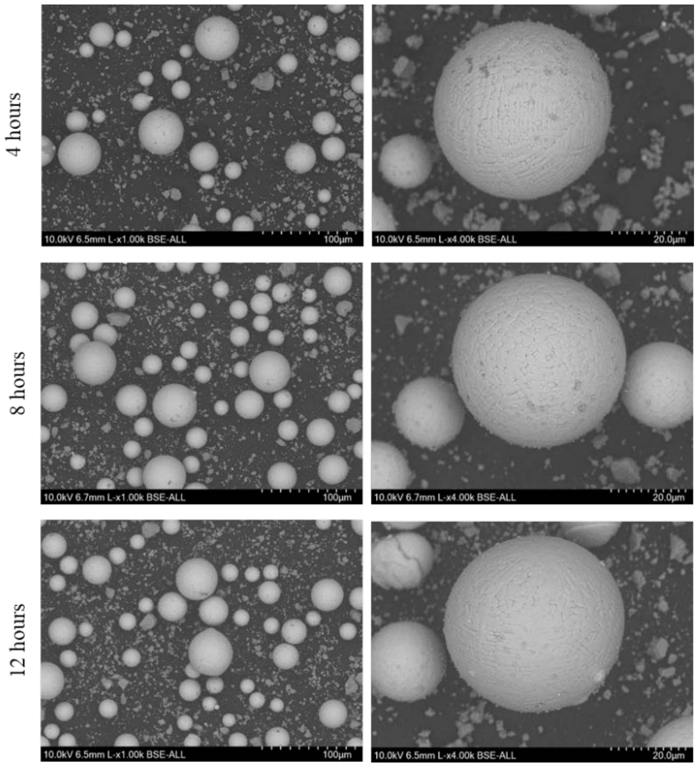

Figure 5. SEM images of 2 wt% micro-sized TiC/Inconel 625 composite powder from the different mixing time and magnification (Turbula system).

Figure 6 shows the morphology and particle shape of 2 wt% nano-sized TiC/Inconel 625 composite powders processed via resonant acoustic under varying mixing times at constant g-force. The results indicate that nano-sized TiC particles were uniformly distributed throughout the matrix without any agglomeration. The spherical morphology of the matrix particles was preserved since there was no mechanical impact during the process. During the initial mixing periods of 3, 4, and 5 min, partial surface attachment of TiC particles to the Inconel 625 matrix was observed; however, some regions remained insufficiently coated. After 6 min of mixing, a significant improvement in adhesion between TiC particles and Inconel 625 matrix was observed as shown in Figure 7. This suggests that 6 min of processing represents the optimal mixing time for achieving uniform dispersion and effective coating of the reinforcement particles.

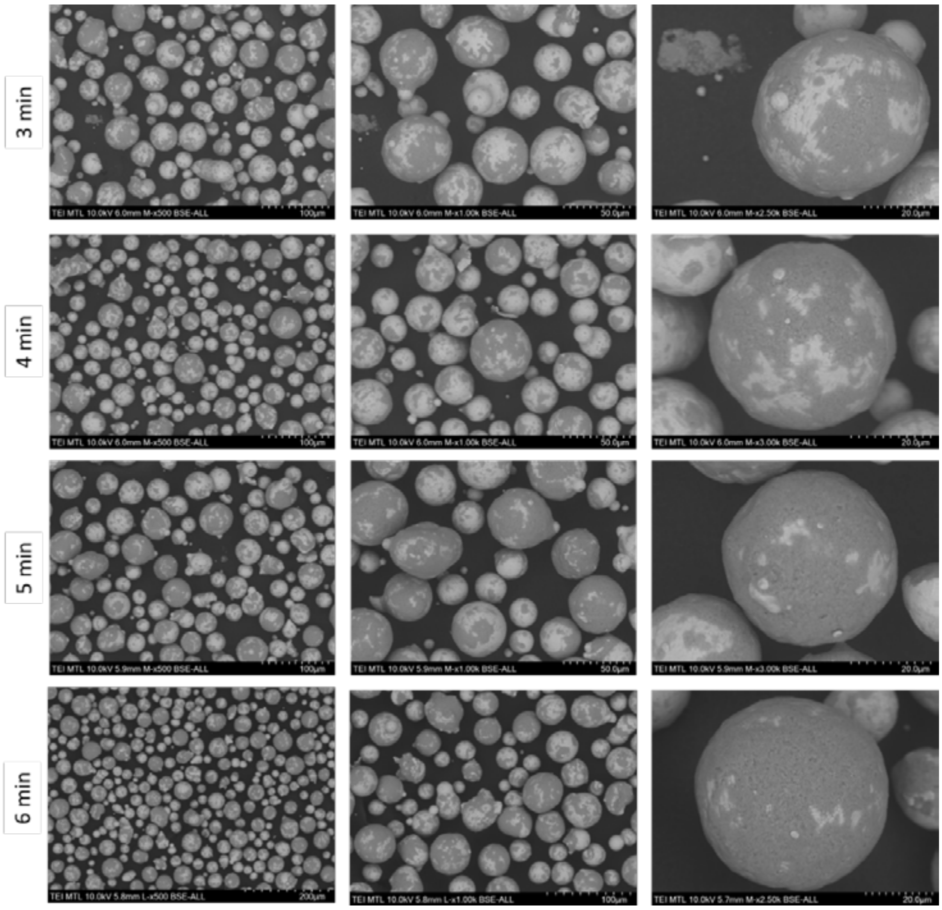

Figure 6. SEM images of 2 wt% nano-sized TiC/Inconel 625 composite powder (RAM) prepared at different mixing time.

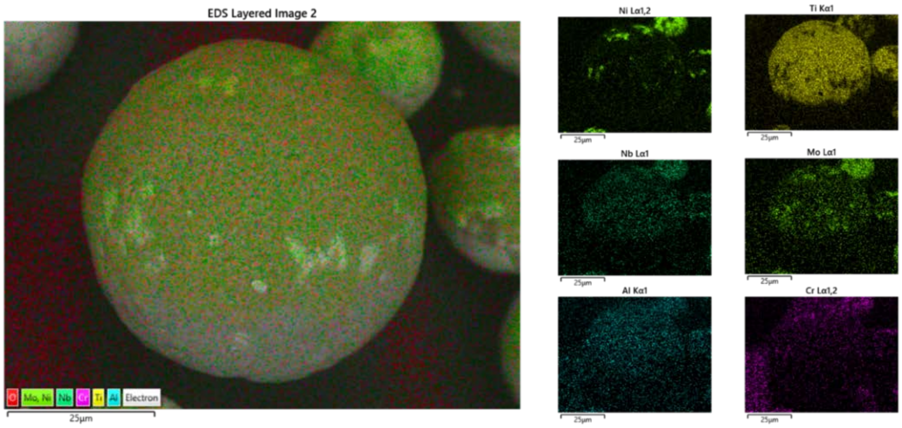

Figure 7. EDS mapping images of 2 wt% nano-sized TiC/ Inconel 625 composite powder prepared (RAM) at 6 min mixing time.

As anticipated, micro-sized TiC particles exhibited, different mixing behaviour compared to their nano-sized counterparts. Owing to their irregular morphology and interparticle van der Waals interactions, micro-sized TiC particles showed a pronounced tendency to agglomerate.

As shown in Figure 8, after 1 min of mixing, although some reinforcement particles were observed on the matrix surface, a significant fraction had already formed agglomerates on the carbon band. However, with extended mixing time, the distribution of micro-sized TiC particles became more uniform, and greater adherence to the matrix particle surfaces was achieved. In contrast to nano-sized TiC particles, the primary challenge for micro-sized TiC reinforcements was minimizing interparticle agglomeration rather than achieving complete surface coverage of the matrix. This observation suggests that mixing strategies for micron-sized reinforcements should prioritize dispersion stability over surface coating efficiency.

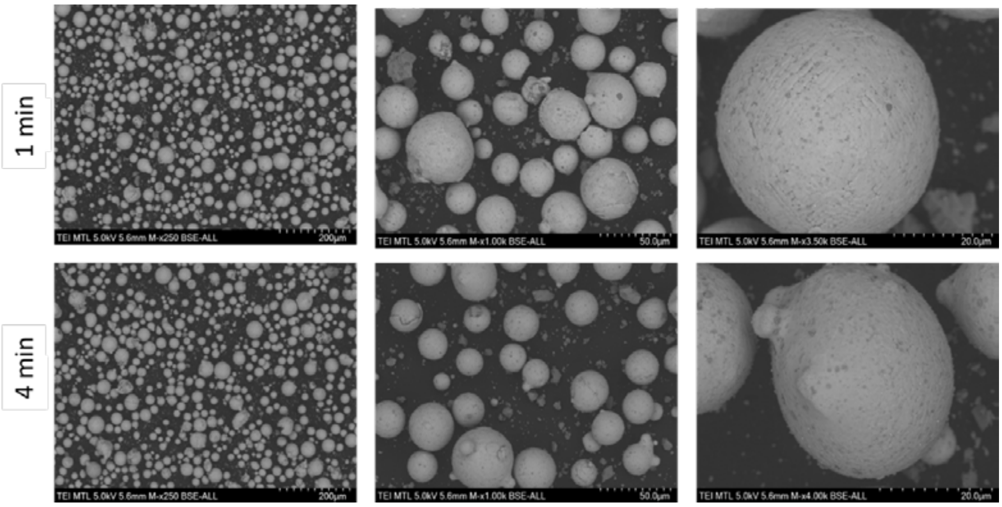

Figure 8. SEM images of 2 wt% micro-sized TiC/Inconel 625 composite powder prepared (RAM) at different mixing.

The apparent density, tapped density, Hausner ratio, and Hall flow rate of TiC-reinforced composite powders processed via RAM and ball milling, along with the matrix powder, are presented in Table 5. No flow measurements were obtained for the powder mixed via tumbler mixer, as the powder failed to flow through the funnel during the test, indicating poor flowability. The matrix powder exhibited an apparent density of 4.616 g/cm³ and a tapped density of 5.264 g/cm³, resulting in a Hausner ratio of 1.14. The Hall flow rate was measured at 17.106 s, both of which indicate good powder flow characteristics.

As shown in Table 5, the flow behaviour of TiC-reinforced composite powders prepared by ball milling is slower compared to the matrix powder, with flow rate decreasing as the reinforcement particle size decreases. The nano-sized TiC/Inconel 625 composite powder exhibited an apparent density of 3.5 g/cm³ and a tapped density of 4.1 g/cm³. The corresponding Hausner ratio was 1.17, and the Hall flow rate was measured as 25.2 s, indicating fair flowability. In contrast, the micro-sized TiC/Inconel 625 composite powder showed higher apparent and tapped densities of 4.2 g/cm³ and 5.0 g/cm³, respectively, with a Hausner ratio of 1.19 and a Hall flow rate of 24.1 s, showing fair flowability. These results indicate that even though both composite powders show reasonable flow properties, the nano-sized TiC/Inconel 625 composite powder indicates slightly poor flow characteristics, likely due to increased interparticle cohesion and surface area.

On the other hand, 2 wt% micro-sized TiC/Inconel 625 composite powder prepared via RAM exhibited an apparent density of 4.508 g/cm^3 and tap density of 5.449 g/ml. The calculated Hausner ratio was 1.208, and the Hall flow rate was measured as 25.014 s, indicating fair flowability. Analysis of the tap density values reveals that the micro-sized TiC particles exhibited the highest tap density, followed by the Inconel 625 matrix powder, while the nano-sized TiC particles showed the lowest value. This behaviour for micro-sized TiC partciles can be attributed to the insufficient adhesion to the matrix. In contrast, the strong adhesion of nano-sized TiC particles to the matrix prevents such separation, resulting in more efficient particle packing. The flowability of the composite powder consisting of an Inconel 625 matrix and nano-sized TiC particles was found to be favourable, whereas the composite powder containing micro-sized TiC particles exhibited slightly reduced flowability but remained within acceptable limits. These results suggest that the insufficient adhesion of micro-sized TiC particles adversely affects the flow behaviour of the composite powder, whereas the nano-sized TiC particles exhibits no detrimental impact on flow properties.

Table 5. Density and flow characteristics of powders (values correspond to composite powder mixtures prepared using optimized mixing parameters).

Mixing method	Sample	Apparent Density (g/cc)	Tap Density (g/ml)	Hausner Ratio	Flow Character	Hall Flow Rate (50g/s)
-	Inconel 625	4.616	5.264	1.14	Good	17.106
Acoustic	µm-TiC composite	4.508	5.449	1.208	Fair	25.014
Acoustic	nm-TiC composite	4.334	4.965	1.145	Good	16.606
Ball Mill	µm-TiC composite	4.2	5	1.19	Fair	24.1
Ball Mill	nm-TiC composite	3.5	4.1	1.17	Good	25.2
Tumbler	nm-TiC composite	Test could not be performed				
Tumbler	µm-TiC composite	Test could not be performed				

Figure 9 shows that the apparent density of Inconel 625 decreases upon reinforcement with TiC particles This can be attributed to the influence of reinforcement particles on powder packing characteristics. However, the RAM method provides higher apparent density compared to both ball milling and tumbler mixing. This improvement is attributed to more uniform dispersion and enhanced interfacial interaction between the matrix and reinforcement particles.

As shown in Figure 10, Hall flow rates for the Inconel 625 matrix and nano-sized TiC/Inconel 625 composite powders processed via RAM are higher than those for micro-sized TiC/Inconel 625 composite powders, while powders prepared by ball milling and tumbler mixing exhibit significantly slower flow rates. This difference is primarily due to uniform particle dispersion and preserved spherical morphology achieved through RAM. In contrast, ball milling induces surface deformation and particle flattening, which negatively affect the flowability.

Figure 11 presents the tapped density results, which follow a trend similar to the apparent density trend observed in Figure 9. The nano-sized TiC/Inconel 625 composite powder processed via RAM exhibits the highest tapped density, indicating improved particle packing efficiency. This is due to minimized agglomeration and improved interfacial contact between the reinforcement and matrix, resulting in more efficient particle arrangement.

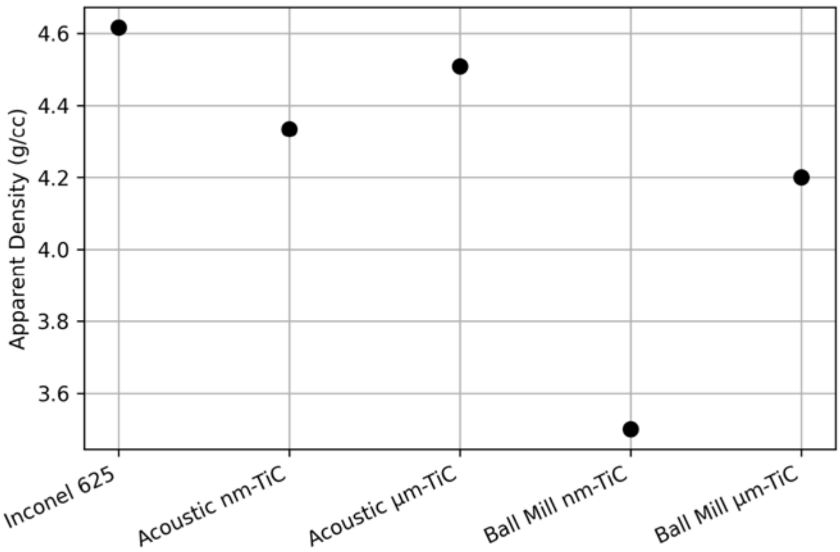

Figure 9. Apparent density of samples by mixing methods.

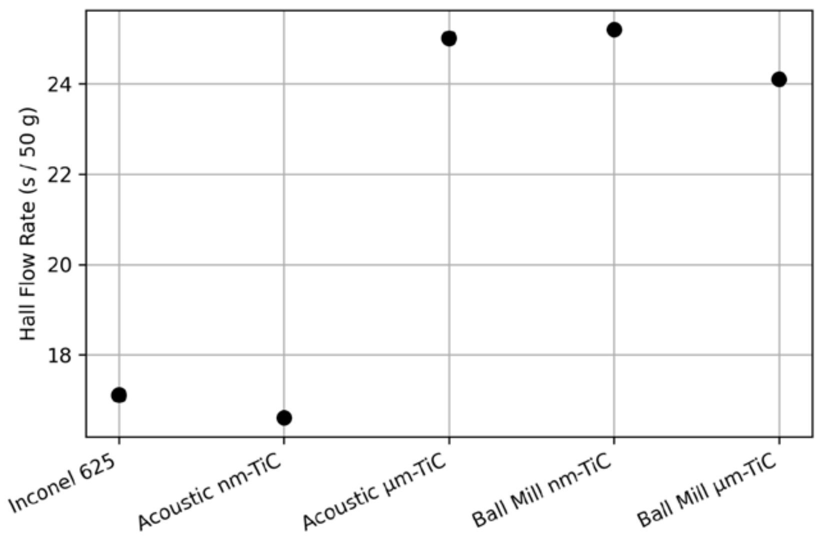

Figure 10. Hall Flow Rates density of samples by mixing methods.

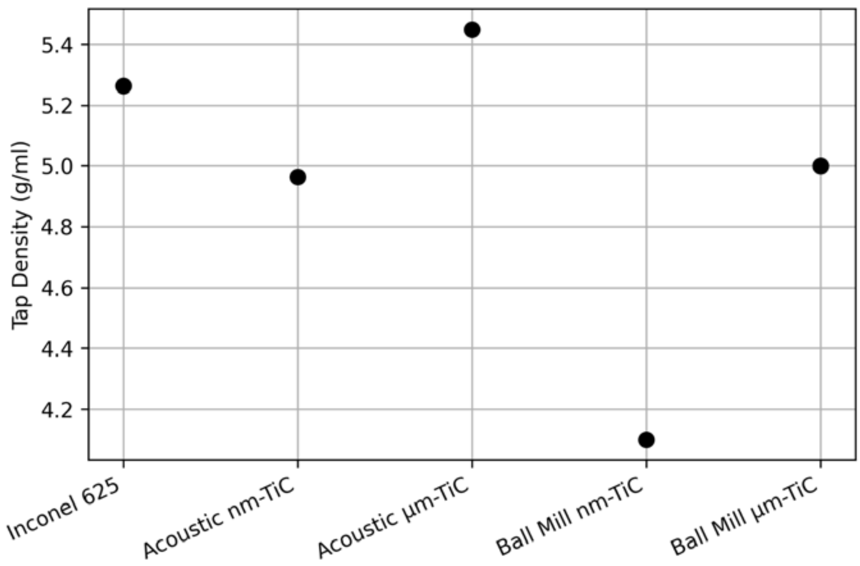

Figure 11. Tap density of samples by mixing methods.

In summary, Table 6 compares different mixing methods for MMC powders and demonstrates that RAM provides enhanced particle dispersion in shorter processing times, along with improved powder flow properties.

Table 6. Comparative chart of mixing methods for MMC powders.

Parameter	Resonant Acoustic Mixing	Ball Milling	Tumbler Mixing
Mixing time	1-6 min	1-3 h	4-12 h
Homogeneity	Minimal agglomeration	Partial dispersion	Visible clustering
Agglomeration	Minimal	Moderate	High
Particle morphology	Preserved	Deformation observed	Preserved
Flow properties (Hausner ratio)	Good (1.145-1.208)	Fair (1.17-1.19)	Fair (1.208)

Figure 12 shows the microstructure of the bulk Inconel 625 matrix sample, revealing distinct melt pools with dendritic features exhibiting a cellular morphology that are generally distributed in a homogeneous manner. Variations in local cooling rates during the additive manufacturing process resulted in dendritic structures aligned parallel to the solidification direction in some regions, while exhibiting a more perpendicular orientation in others. No gas porosity was observed within the microstructure. EDS analysis confirmed the chemical composition of the material, with no detectable signs of contamination.

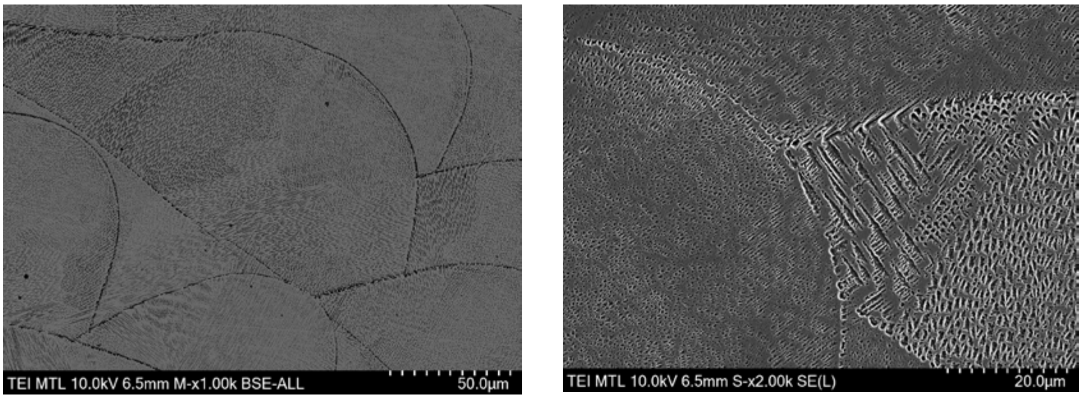

Figure 12. SEM images of the bulk Inconel 625 matrix.

Figure 13 shows that, similar to the Inconel 625 matrix, distinct melt pools were observed in the bulk nano-sized TiC/Inconel 625 composite sample. The nano-sized TiC particles acted as effective nucleation sites, promoting the formation of equiaxed grains instead of the typical columnar dendritic structures. This grain refinement is consistent with established literature, where ceramic reinforcements such as TiC are known to enhance nucleation and suppress columnar growth (Al Mangour et al., 2007). However, EDS analysis revealed localized agglomeration of nano-sized TiC particles within the microstructure, suggesting incomplete dispersion despite their role in grain refinement.

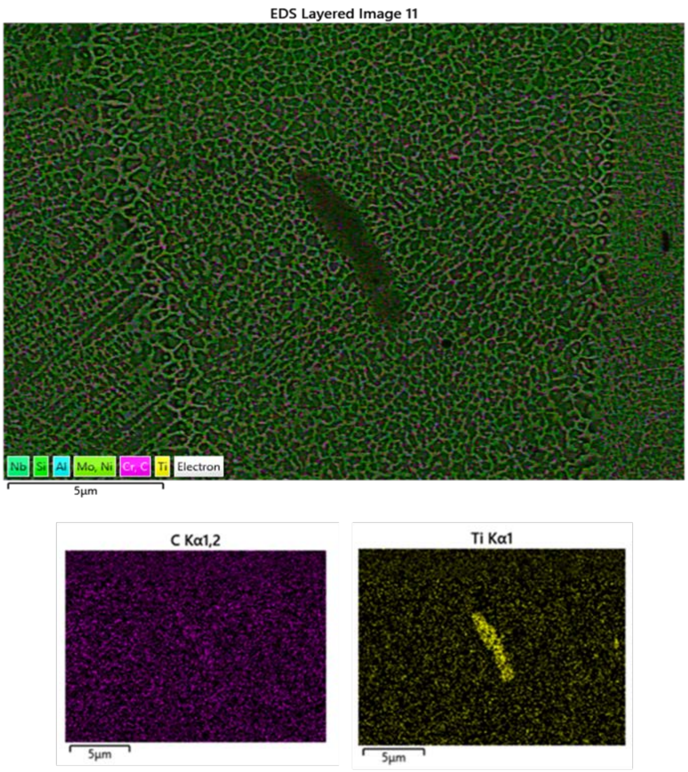

Figure 13. SEM-EDS images of the bulk nano-sized TiC/Inconel 625 sample.

Figure 14 shows distinct melt pools within the microstructure of micron-sized TiC/Inconel 625 bulk sample, with EDS analysis revealing the presence of agglomerations. These agglomerations are significantly higher compared to the nano-sized TiC/Inconel 625 bulk sample and distributed throughout the matrix and primarily attributed to their larger particle size. Moreover, it can be seen that unmelted or partially melted micron-sized particles were located near the melt pool boundaries during processing, where they accumulate and form agglomerates.

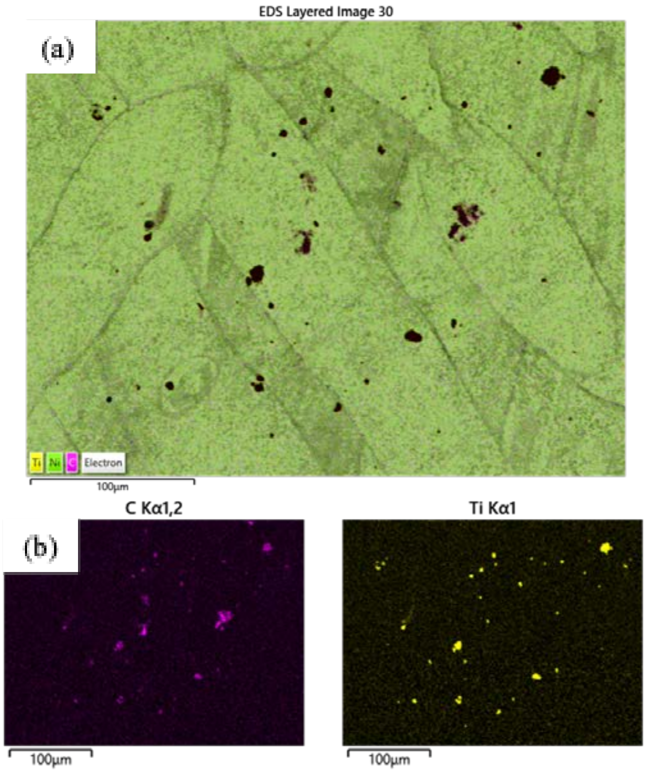

Figure 14. (a) SEM images and (b) EDS analysis of the bulk micro-sized TiC/Inconel 625 sample.

As shown in Table 7, the Inconel 625 matrix exhibited average hardness values of 24 HRC in the Z-direction and 23 HRC in the XY-direction. Both bulk TiC particles-reinforced composite samples achieved higher average hardness values compared to the unreinforced matrix, indicating a substantial improvement in mechanical resistance. This enhancement is primarily attributed to effective load transfer from the ductile Inconel 625 matrix to the hard, rigid TiC particles, as well as contributions from grain refinement and dispersion strengthening mechanisms.

Table 7. Comparative macro-hardness chart.

Material	Z-direction	XY-direction
Inconel 625 matrix	24	23
2 wt% micro-sized TiC/Inconel 625	35	35
2 wt% nano-sized TiC/Inconel 625	33	34

4. Discussion

These findings show that composite powder flow properties may substantially depend on mixing method regardless of the reinforcement particles (nano- or micro-scale size). Meanwhile, achieving strong adhesion between the reinforcement particles and the matrix powder is critical for maintaining powder integrity during LPBF, where optimal flowability and consistent powder deposition are essential for quality of final part. The results showed that mixing methods such as ball milling and tumbler mixing produced composite powders with poor flow characteristics, while RAM provided improved flowability due to the ability to homogeneously disperse TiC particles in the Inconel 625 matrix without compromising spherical powder morphology.

In the case of nano-sized TiC/Inconel 625 composite powders, tumbler mixing resulted in pronounced agglomeration, with no significant improvement observed even after extended mixing durations. Similarly, ball milling was unable to achieve fully homogeneous mixing despite variations in rotational speed and mixing time. In contrast, RAM proved to be highly efficient, achieving homogeneous particle dispersion and strong adhesion to the matrix within only 3 min, with no evidence of agglomeration.

Considering micro-sized TiC/Inconel 625 composite powders, while the mixtures exhibited slight changes in uniformity, tumbler mixing had limited effectiveness since even at longer mixing duration. However, the ball milling method managed improved homogeneity than tumbler mixing, where higher rotational speed and longer duration enhanced the mixing quality. Nevertheless, RAM accomplished more uniform distribution compared to both alternatives, and longer mixing duration further improved dispersion quality. Among the methods tested, RAM provided the most effective and homogeneous mixing for micro-sized TiC particles.

The addition of TiC particles promotes the alteration in microstructure from columnar to equiaxed grain structures. Although agglomeration is observed in bulk samples with both nano- and micro-sized TiC particles, it is more noticeable in specimens reinforced with micro-sized particles. TiC usually does not melt during processing owing to its high melting point. Due to its high melting point, TiC typically does not melt during processing; however, partial dissolution may occur when particle size is reduced to the nanoscale, combined with low TiC content. In nano-sized TiC particles-reinforced specimens, agglomeration is primarily driven by the relatively low density of TiC particles, which promotes their flotation within the melt pool. During rapid solidification, these floating particles tend to segregate toward melt pool boundaries, where they accumulate and form agglomerates. In contrast, agglomeration in micro-sized TiC particles-reinforced specimens is mainly attributed to the larger particle size, the inability of the particles to melt, and insufficient interfacial bonding with the matrix.

Among the powder mixing techniques investigated, RAM has emerged as a promising method for achieving rapid and uniform particle dispersion. Compared to ball milling, which may deform the powder morphology, or tumbler mixing, which often requires extended processing times, acoustic mixing offers a balance between processing efficiency and powder quality. This method is particularly effective for nano-sized reinforcements, as it minimizes agglomeration while preserving the original morphology of the particles.

5. Conclusion

This study aimed to uniformly disperse 2 wt% TiC particles with different sizes in Inconel 625 matrix powders using the various mixing techniques. Among the methods tested, RAM achieved homogeneity in short time, maintaining the spherical morphology of the matrix particles. The flow properties of the RAM-prepared powders remained at optimal levels, as a result of low Hausner ratio (1.145) and Hall flow rate (16.6 g/s). These characteristics ensures that composite powders suitable for LPBF. Ball milling resulted in partial improvement in reinforcement dispersion but introduced surface deformation and agglomeration. These effects decreased the powder flowability apparent and tap and density. Tumbler mixing preserved particle morphology but failed to disperse agglomeration, even with extended mixing times (4-12 hours). Additionally, the TiC particles showed poor adhesion to the matrix. The samples produced with LPBF using the powders created with RAM showed low level of porosity. Due to the small size of the TiC nano-sized particles, they acted as nucleation sites for the equiaxed grain growth. On the other hand, the micro-sized TiC particles agglomerated due to their shape and size. The reinforcement of 2 wt% TiC into Inconel 625 matrix significantly enhanced hardness around 47%. The RAM mixing technique was found to be the most effective method in this study since it produced high-quality composite powders within the shortest time possible. RAM has proved its effectiveness as an ideal method for producing MMC powders, which can be used in LPBF technology.

Conflict of Interest

The authors declare no conflict of interest

Author Contributions

Dursun, G. devised the project and main conceptual. Celik, D., Gundogan, Y.C., and Bal, İ carried out the experiments. Dursun, G., Celik, D., Gundogan, Y.C., and Bal, İ. wrote the article.

Funding

This research was supported by Secretariat of Defence Industries (SSB).

Acknowledgments

Authors would like to express sincere gratitude to Secretariat of Defence Industries (SSB) and Tusas Engine Industries (TEI) for all supports throughout the current study.

References

AlMangour, B., Grzesiak, D. & Yang, J. (2007). Scanning strategies for texture and anisotropy tailoring during selective laser melting of TiC/316L stainless steel nanocomposites. *Journal of Alloys and Compounds, 728*, 424-435, https://doi.org/10.1016/j.jallcom.2017.08.022.

Baitimerov, R., Lykov, P., Zherebtsov, D., Radionova, L., Shultc, A., & Prashanth, K. G. (2018). Influence of Powder Characteristics on Processability of AlSi12 Alloy Fabricated by Selective Laser Melting. *Materials*, *11*(5), 742. https://doi.org/10.3390/ma11050742.

Dadbakhsh, S., Mertens, R., Vanmeensel, K., Ji, G., & Kruth, J. P. (2020). In situ transformations during SLM of an ultra-strong TiC reinforced Ti composite. *Scientific Reports, 10*, https://doi.org/10.1038/s41598-020-67434-3.

Gorji, N. E., O'Connor, R., Mussatto, A., Snelgrove, M., González, P. M., & Brabazon, D. (2019). Recyclability of stainless steel (316 L) powder within the additive manufacturing process. *Materialia, 8,* https://doi.org/10.1016/j.mtla.2019.100489.

Gu, D., Wang, Z., Shen, Y., Li, Q., & Li, Y. (2009). In-situ TiC particle reinforced Ti–Al matrix composites: Powder preparation by mechanical alloying and Selective Laser Melting behavior. *Applied Surface Science, 255*(22), 9230–9240. https://doi.org/10.1016/j.apsusc.2009.07.008.

Liu, B., Wildman, R., Tuck, C., Ashcroft, I., & Hague, R. (2011). Investigation the effect of particle size distribution on processing parameters optimisation in selective laser melting process. *Additive manufacturing research group, Loughborough University*, 227-238.

Murray, J. W., Simonelli, M., Speidel, A., Grant, D. M., & Clare, A. T. (2019). Spheroidisation of metal powder by pulsed electron beam irradiation. *Powder Technology*, *350*, 100–106. https://doi.org/10.1016/j.powtec.2019.03.041.

Niu, H. & Chang, I. (1999). Selective laser sintering of gas and water atomized high speed steel powders. *Scripta Materialia, 41*(1), 25-30. https://doi.org/10.1016/s1359-6462(99)00089-5.

Parsons, E. M. & Shaik, . S. Z. (2022). Additive manufacturing of aluminum metal matrix composites: Mechanical alloying of composite powders and single track consolidation with laser powder bed fusion, *Additive Manufacturing, 50*, https://doi.org/10.1016/j.addma.2021.102450.

Poyraz, O. & Kushan, M. (2019). Residual Stress-induced Distortions in Laser Powder Bed Additive Manufacturing of Nickel-based Superalloys. *Journal of Mechanical Engineering, 65*(6), 343-350. http://dx.doi.org/10.5545/sv-jme.2019.6004.

Smith, T. M., Thompson, A. C., Gabb, T. P., Bowman, C. L., & Kantzos, C. A. (2020). Efficient production of a high-performance dispersion strengthened, multi-principal element alloy. *Scientific Reports, 10*(1), https://doi.org/10.1038/s41598-020-66436-5.

Thompson, P., Poveda, R., Bezsonov, I., Rossini, M., Orthner, D., Cobb, K., ... & Iqbal, Z. (2019). *AlSi10Mg Nanocomposites Prepared by DMLS Using In-Situ CVD Growth of CNTs: Process Effects and Mechanical Characterization.* , Orthner, D., Cobb, K., Leng, B., Iqbal, Z., (pp. 41-46). Cham: Springer International Publishing.

Tjong, S. C., 2007. Novel Nanoparticle-Reinforced Metal Matrix Composites with Enhanced Mechanical Properties. *Advanced Engineering Materials,* 9(8), 639–652. https://doi.org/10.1002/adem.200700106.

Yang, G., Xie, Y., Zhao, S., Ren, Y., & Wang, C. (2022). Methods and Mechanism of Powder Mixing for Selective Laser Melting. *Manufacturing Technology,* 22(1), 102–110. https://doi.org/10.21062/mft.2022.006.

Yao, X., Moon, S. K., Lee, B. Y. & Bi, G. (2017). Effects of heat treatment on microstructures and tensile properties of IN718/TiC nanocomposite fabricated by selective laser melting. *Int. J. Precis. Eng. Manuf, 18,*1693–1701. https://doi.org/10.1007/s12541-017-0197-y.

Zhai, W., Zhou, W., Nai, S. M. L. & Wei, J. (2020). Characterization of nanoparticle mixed 316 L powder for additive manufacturing. *Journal of Material Science and Technology,* Volume 47, 162–168. https://doi.org/10.1016/j.jmst.2020.02.019.

Zhuang, J., Gu, D., Xi, L., Lin, K., Fang, Y., & Wang, R. (2020). Preparation method and underlying mechanism of MWCNTs/Ti6Al4V nanocomposite powder for selective laser melting additive manufacturing. *Powder Technology, 368,* 59-69. https://doi.org/10.1016/j.powtec.2020.04.041.